Appendix F
Structural Analysis Models

1.0 Introduction

To investigate the cable failures and eventual collapse of the telescope, it is necessary to determine how the cable tensions varied over time when the telescope was operating and subject to environmental loads such as temperature, wind, and earthquakes. To perform this analysis, we constructed finite element analysis (FEA) models of the original and upgraded telescope structures. Analysis was primarily performed in the FEA program SAP2000, and some analyses were repeated in the FEA program Abaqus for validation. All of the FEA models used are based on similar assumptions and are of similar scope and level of detail.

The assumptions made in the FEA models are presented in this appendix. The general structural behavior of the telescope, as determined from the models, is also presented. The models were then used to determine the cable tensions under a variety of loads, and these results are presented in Appendix G, H, I, J and K.

2.0 Modeling Assumptions

The assumptions below were used to build the telescope models in both FEA programs.

2.1 Elements and Boundary Conditions

The FEA models are built to represent the superstructure of the telescope, which includes the towers, suspended structure, mains, backstays, tiedowns and waveguide. The telescope's primary reflector and ground screen are structurally independent of the superstructure and are not included in these analysis models. Distinct models were built to analyze the original structure (Figure 1) and the upgraded structure (Figure 2).

The **towers** are modeled as frame elements, which capture axial, shear, bending and torsional deformations, as well as P-delta effects in nonlinear analyses. The stepped shape of the towers is modeled using several frame elements of different cross-sections. The bottom of each tower is assumed to be fully fixed and located at the elevation of the top of the tower pedestal.

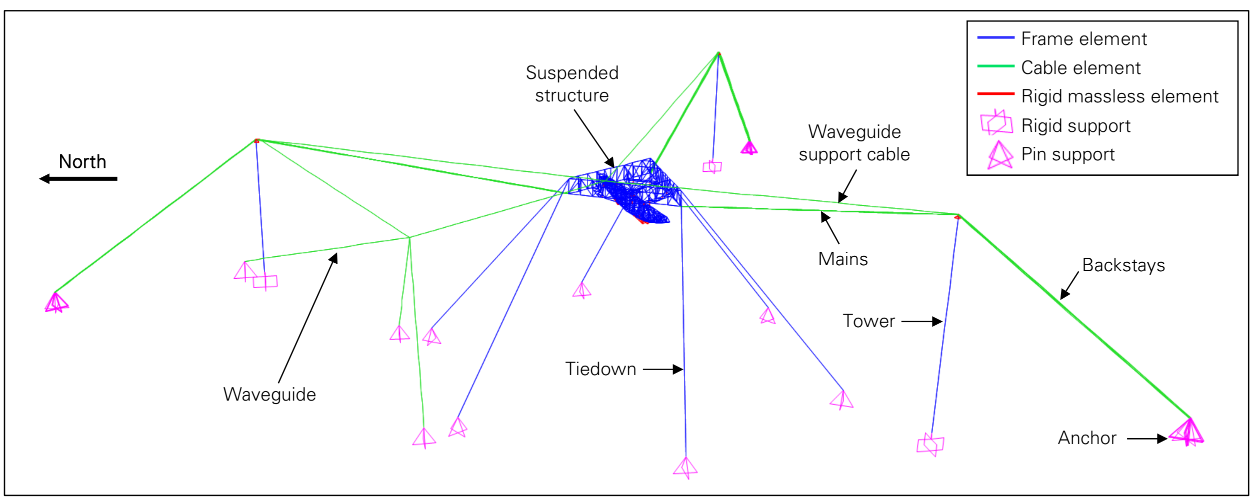

Figure 1: Finite element model of original structure.

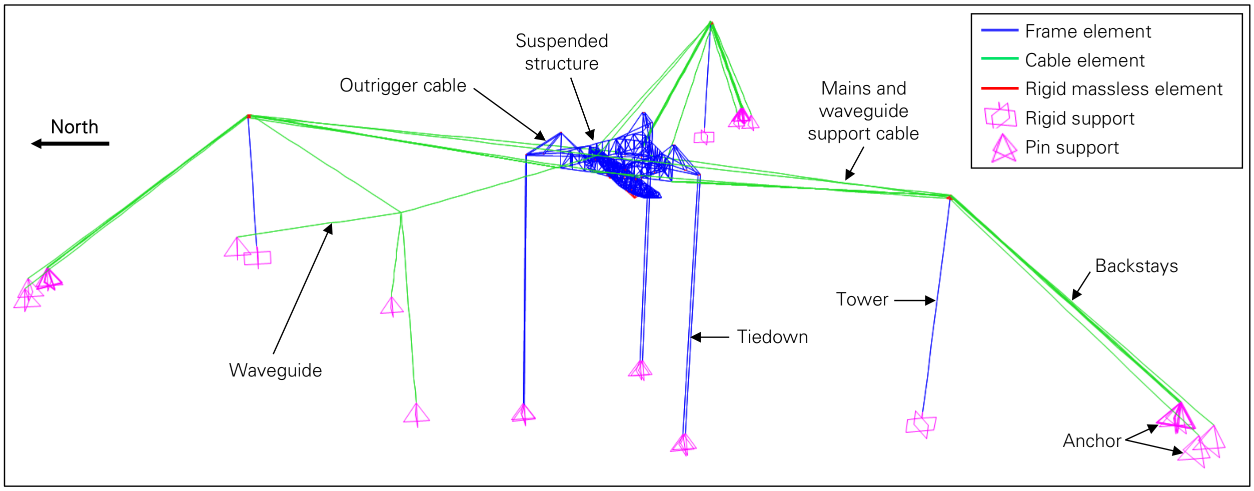

Figure 2: Finite element model of upgraded structure.

The platform and azimuth arm trusses of the **suspended structure** are also modeled as frame elements. These truss members are built up from standard steel channels and angles with lacing. We assume that the lacing is rigid, such that the channels and angles act compositely. Because the azimuth arm is modeled in the stowed position, which the telescope was locked in before high wind events, we apply wind loads directly to the azimuth arm in our wind analyses (Appendix J). To model other positions of the azimuth arm during telescope operation, the azimuth arm elements can be removed from the model and replaced with equivalent gravity loads that act directly on the platform (Appendix H). The steel cables in the outriggers of the upgraded platform are short in length and tensioned adequately such that their sags are negligible. These cable elements are therefore also modeled as frame elements.

The **Gregorian** and **line feed(s)** are not primary structural elements, and they are not modeled as finite elements in the suspended structure. Their weight is applied to the azimuth arm in accordance with their positions.

The **mains and backstays** are modeled as cable elements, whose behavior take into account the cable sag. Although the cable elements used in the SAP2000 and Abaqus models do not have identical assumptions, both versions of those elements are adequate for the analysis of the telescope structure. This is further discussed in sections 3.0 and 4.0 below. The **waveguide**, waveguide support cables and waveguide tiedowns are also modeled as cable elements.

Even though the **tiedowns** of the suspended structure are steel cables, these cables are modeled as frame elements because their sag is negligible: the tiedowns of the upgraded structure are vertical, while the tiedowns of the original structure were inclined but supported by carrier cables. Carrier cables were only installed during the first upgrade in 1974. Since this first upgrade did not significantly impact the telescope’s structural behavior, the pre-1974 structure is not modeled in our analysis.

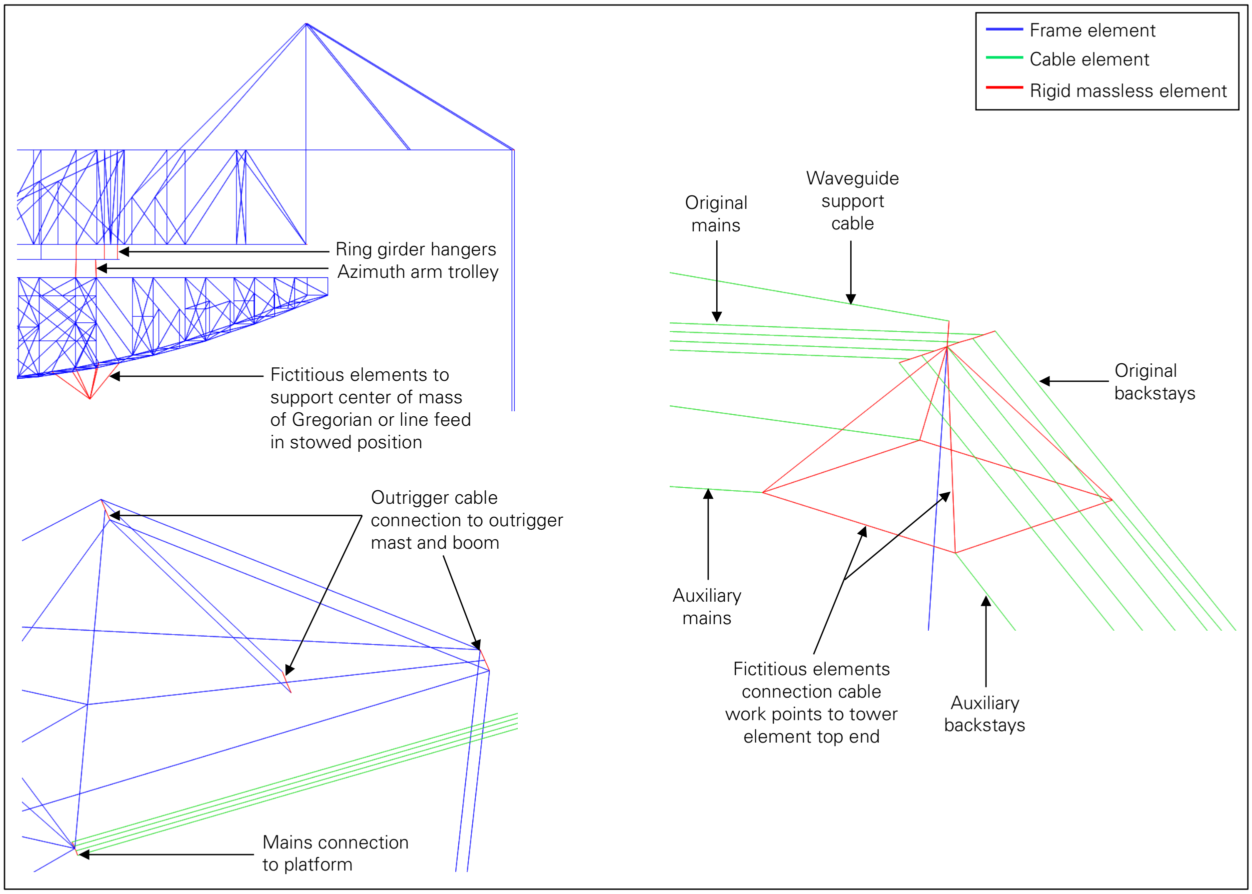

Figure 3: Use of rigid massless elements.

As shown in Figure 3, some of the frame and cable elements are connected in the model with rigid massless elements. Rigid massless elements are used to model some of the cable connections to the towers and the platform, so that each cable element starts and ends at the work point of the actual cable. Rigid massless elements are also used to model the ring girder hangers and azimuth arm trolleys due to their rigidity and short length. Finally, rigid massless elements are used to add a node at the actual center of mass of the Gregorian and line feed(s) in each model, so that the mass distribution of the suspended structure can be accurately modeled in dynamic analyses.

2.2 Concrete Properties

The weight and stiffness of the concrete towers contribute the dynamic properties of the structure. The towers were built in the early 1960s and are made of normal-weight reinforced concrete, which we assume to weigh 150 pounds per cubic foot (pcf).

After the collapse of the telescope, concrete cores were taken at multiple points on the towers while installing scaffolding, and the cores were tested for strength, with the test results presented in Table 1. The average strength varies from 5.71 kilopound per square inch (ksi) to 6.43 ksi between the towers. Based on these results, we assume a uniform concrete strength of 6 ksi for the structural analysis model. From this assumed strength, the Young's modulus is estimated at 4,415 ksi, per the ACI 318-14 standard.[1]

Table 1: Concrete strength test results.

	Tower 4	Tower 8	Tower 12
Number of Tests	3	33	8
Average Strength [ksi]	6.36	5.71	6.43
Strength Standard Deviation [ksi]	1.36	1.38	0.56
Strength Coefficient of Variation	21%	24%	9%

Our analyses of the structure's response to hurricanes (Appendix J) and earthquakes (Appendix K) indicate that most of the tower concrete did not experience any tension large enough to cause cracking. The concrete stiffness is therefore not reduced in the models.

2.3 Cable Properties

The cable properties are critical parameters in the structural analysis of the telescope. For instance, the cable mechanical properties affect how multiple cables share the environmental loads acting on the suspended structure, and the cable weight is key to the calculation of cable tensions from the results of the sag surveys.

Per the structural drawings for the second upgrade of the telescope (1992), the auxiliary cables met the ASTM A586[2] standard, which specifies the metallic area, Young's modulus, and linear weight for any cable diameter. Samples of the auxiliary cables were also tested at Lehigh University before installation (1993). The original construction drawings (1960) do not specify a standard for the original cables, but they require a minimum wire tensile strength of 220 ksi, consistent with the ASTM A586 standard. The original and auxiliary cables are also of similar fabrication, with galvanized steel wires arranged in alternating helicoid layers to form a single strand.

We considered both the ASTM A586 standard and the 1993 Lehigh tests to select cable properties for the models. For the sake of consistency, we calculated the cable properties from the nominal cable diameter using the same equations and assumptions for every cable, and we verified that the results were consistent with the ASTM A586 and Lehigh test values. This process is summarized in Table 2, which compiles the ASTM values, the Lehigh values (when available), and the values used in the models. Table 2 also provides the coefficient of variation (CV) between the different values: the CV does not exceed five percent, which is satisfactory since a five percent difference in any cable property would not significantly impact the cable and telescope behavior under load.

The **metallic area** of a cable section is modeled as 75 percent of the nominal area, which is directly calculated from the nominal diameter.

The **effective Young's modulus** of the wires is assumed to be 25,500 ksi, which is the average of the two values measured in the Lehigh tests. This is lower than Young's modulus of solid steel (typically

[1] American Concrete Institute. *ACI 318-14. Building Code Requirements for Structural Concrete*, 2014.

[2] American Society for Testing and Materials. *ASTM A586-18. Standard Specification for Metallic-Coated Parallel and Helical Steel Wire Structural Strand*. 2018.

29,000 ksi) because of the helical arrangement of the wires and the softer galvanizing zinc around each wire, though it is higher than the minimum of 23,000 ksi required per ASTM.

The **axial rigidity** of a cable is the product of the effective Young's modulus and the metallic area.

The **linear weight** of a cable is modeled as 79 percent of the weight of a solid steel rod of nominal cable diameter, considering a steel weight density of 490 pcf.

The **minimum breaking strength** has not been calculated but is taken directly from the second upgrade structural drawings, which provide the minimum breaking strength of the new auxiliary cables to be installed during the upgrade, as well as the existing original cables. The actual breaking strength of the auxiliary cables tested at Lehigh in 1993 was measured five to eight percent higher than the minimum specified breaking strength.

Table 2: Selection of cable properties for analysis models. The values used in the models are in **bold**.

	Source	Original Mains	Original Backstays	Auxiliary Mains	Auxiliary Backstays
Nominal Diameter [in]	-	3	3-1/4	3-1/4	3-5/8
Nominal Area [in^2]	-	7.07	8.30	8.30	10.32
Metallic Area [in^2]	ASTM A586	5.4	6.3	6.3	7.9
	1993 Lehigh tests	-	-	6.23	7.65
	Modeled = 0.75 x (nominal area)	**5.30**	**6.22**	**6.22**	**7.74**
	CV	1%	1%	1%	1%
Effective Young's Modulus [ksi]	ASTM A586 (minimum)	23,000	23,000	23,000	23,000
	1993 Lehigh tests	-	-	25,000	25,900
	Modeled = 25,500 ksi	**25,500**	**25,500**	**25,500**	**25,500**
	CV	5%	5%	4%	5%
Axial Rigidity [kip]	ASTM A586	124,200	144,900	144,900	181,700
	1993 Lehigh tests	-	-	155,638	198,115
	Modeled = 0.75 x (nominal area) x (25,500 ksi)	**135,187**	**158,657**	**158,657**	**197,382**
	CV	4%	5%	4%	4%
Linear Weight [lbf/ft]	ASTM A586	19.00	22.00	22.00	28.00
	1993 Lehigh tests	-	-	21.18	26.03
	Modeled = 0.79 x (nominal area) x (490 pcf)	**18.91**	**22.19**	**22.19**	**27.60**
	CV	0%	0%	2%	3%
Minimum Breaking Strength [kip]	1992 upgrade drawings	1,044	1,212	1,314	1,614
	1993 Lehigh tests	-	-	1,414	1,687
	Considered = 1992 upgrade drawings	**1,044**	**1,212**	**1,314**	**1,614**
	CV	0%	0%	3%	2%

2.4 Baseline Cable Tensions

Models are used to perform multiple static and dynamic analyses to determine how cable tensions vary during telescope operation and under environmental loads. Before running any analysis, a model is initialized in a baseline state where the cable tensions are known.

For the original structure, the baseline cable tensions are those determined by Ammann & Whitney before the second upgrade of the telescope. These tensions are specified at the start of the cable jacking sequence for the second upgrade, with the original tiedowns already removed from the structure.

For the upgraded structure, the baseline cable tensions are those in effect when the telescope is in the stowed position, with the tiedowns slack before the first cable failure. To determine these tensions, we began with the August 2020 sag survey that provides reliable values for the cable tensions after the first cable failure, and we removed the effect of the cable failure through analysis. This process is detailed in Appendix G.

The baseline cable tensions for the original and upgraded structures are shown in Figure 4. In both cases, the telescope is stowed, and the tiedowns are slack or removed. The complete baseline states of the models are summarized in section 2.7.

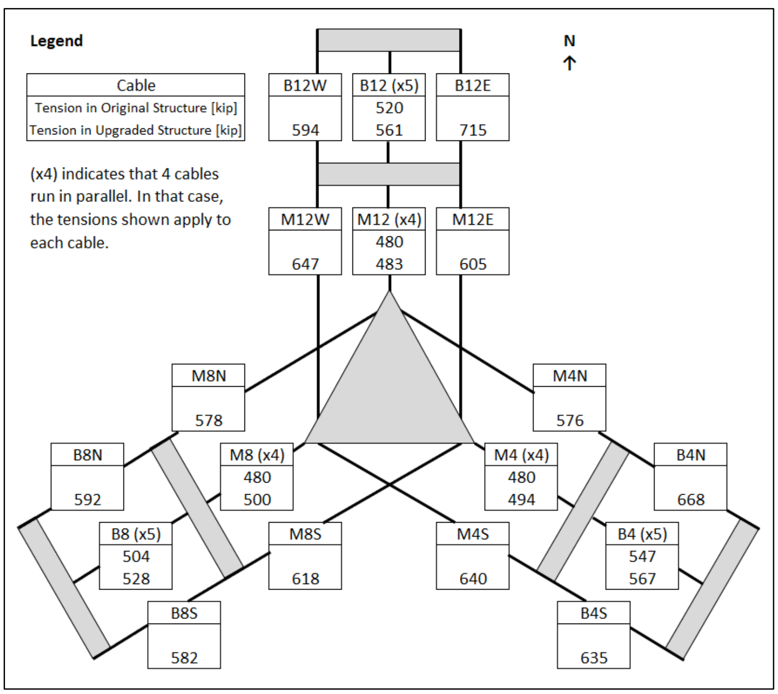

Figure 4: Baseline cable tensions (stowed position and slack tiedowns) in original and upgraded structures.

2.5 Suspended Structure Weight

The weight of the suspended structure changed over time as new equipment was added to the telescope, particularly during the second upgrade with the addition of the Gregorian, counterweight, tiedown outriggers and steel reinforcement. We determined the total weight of the suspended structure at two points in time from the baseline cable tensions described above: from the known cable weights, dimensions and tensions, we calculated the vertical reaction at the platform end of each main cable and added them up to obtain the weight of the suspended structure. The parameters and results of this calculation are shown in Table 3. We calculated a total weight of 1,225 kilopound (kip) for the original structure and 1,825 kip for the upgraded structure. The weight difference (600 kip) is consistent with the 615 kip weight increase indicated in the structural drawings for the second upgrade.

Table 3: Suspended structure total weight calculation from baseline cable tensions.

Main Cable(s)	Qty.	Linear Weight [lbf/ft]	Horiz. Length [ft]	Original Structure				Upgraded Structure			
				Vert. Length [ft]	Horiz. Force [kip]	Average Tension [kip]	Vert. Force on Platform [kip]	Vert. Length [ft]	Horiz. Force [kip]	Average Tension [kip]	Vert. Force on Platform [kip]
M4	4	18.91	575	132	468	480	102	130	482	494	104
M4N	1	22.19	711	-	-	-	-	126	568	576	92
M4S	1	22.19	711	-	-	-	-	126	630	640	103
M8	4	18.91	575	132	468	480	102	130	488	500	105
M8N	1	22.19	711	-	-	-	-	126	569	578	92
M8S	1	22.19	711	-	-	-	-	126	608	618	99
M12	4	18.91	575	132	468	480	102	130	471	483	101
M12E	1	22.19	711	-	-	-	-	126	596	605	97
M12W	1	22.19	711	-	-	-	-	126	638	647	105
Total	-	-	-	-	-	-	1,225	-	-	-	1,825

In the structural analysis models, the weight of the suspended structure is broken down as shown in Table 4 and illustrated in Figure 5 and Figure 6.

The weight for the structural steel of the platform and azimuth arm is estimated to be 1,085 kip by applying a factor of 1.5 to the weight of the frame elements. This factor is estimated from typical member and connection designs to account for the weight of member lacing and connections, which are not explicitly modeled. Some of the platform and azimuth arm members were reinforced during the second upgrade and, for the sake of simplicity, the properties of these reinforced members are used in all the models. Even though the weight of the structural steel is slightly overestimated in the models of the original structure, it does not significantly impact the analysis because the total weight of the suspended structure is correctly modeled by adjusting the superimposed dead load.

The weight of the Gregorian, line feed and/or second carriage house is modeled as concentrated loads at the center of mass of the respective objects. As shown in Figure 5 and Figure 6, rigid massless elements are used to tie each center of mass to the azimuth arm. The counterweight is assumed to be evenly shared by the four azimuth arm work points that support the actual counterweight tray.

Finally, a superimposed dead load is calculated to obtain the total weight determined from the baseline cable tensions. This dead load is evenly distributed between the work points of the middle span of the azimuth arm, as this is where most of the telescope's additional equipment (electrical, mechanical, catwalks, etc.) is located.

Table 4: Suspended structure weight breakdown in FE models.

	Weight in Model of Original Structure [kip]	Weight in Model of Upgraded Structure [kip]
Platform + Azimuth Arm Structural Steel	1,085	1,085
Outriggers + Slack Tiedowns	-	51
Line Feed	35	35
Second Carriage House	35	-
Gregorian	-	200
Counterweight	-	45
Superimposed Dead Load	70	410
Total	1,225	1,825

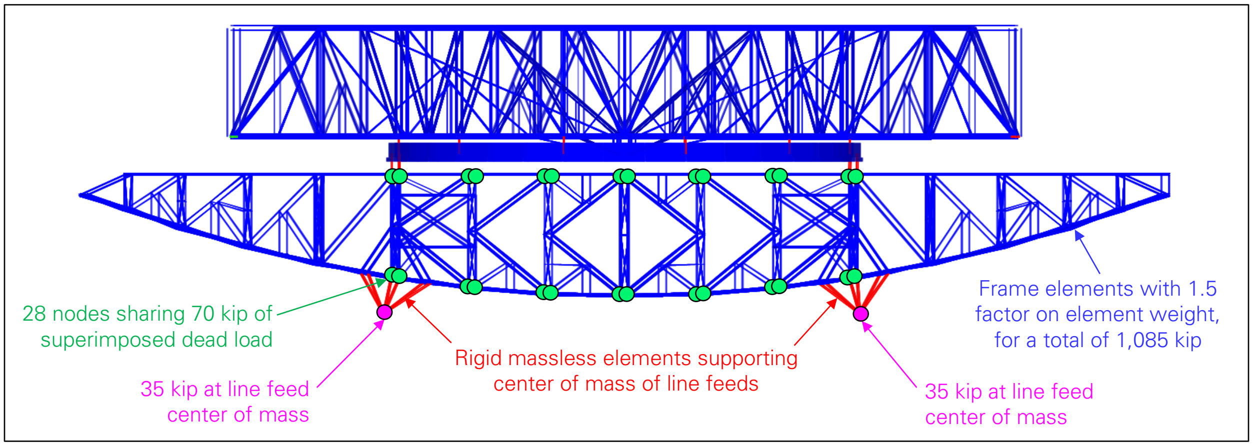

Figure 5: Weight distribution in FEA model of original suspended structure.

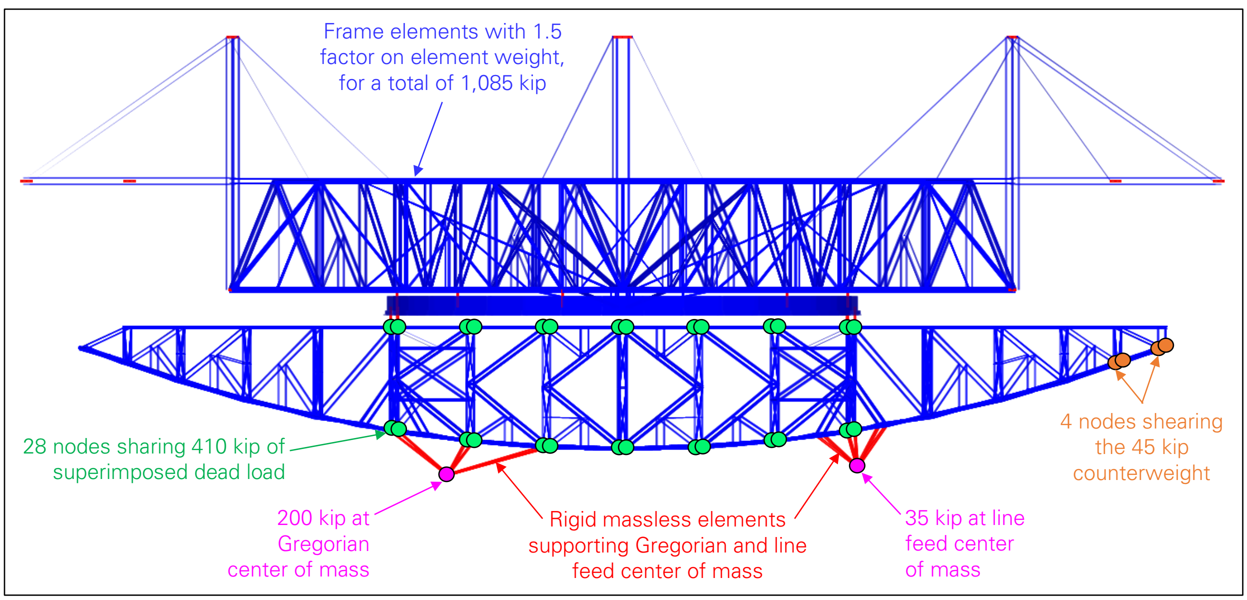

Figure 6: Weight distribution in FEA model of upgraded suspended structure.

2.6 Damping

The global vibration modes of the telescope involve movement of the towers and the suspended structure (section 6.0 below). The structure does not include an engineered damping system to mitigate global vibrations that may be induced by dynamic environmental loads such as wind and earthquakes. The mains and backstays are equipped with Stockbridge dampers (Figure 7), but these dampers are specifically tuned to mitigate cable vibrations and do not act on the global movement of the structure. As a result, the global vibrations are only controlled by the telescope structure's intrinsic damping, which is due to several phenomena, such as friction in the bolted steel connections of the platform, between the layers of cable wires, or within the reinforced concrete of the towers.

Figure 7: Stockbridge dampers on Tower 4 original mains.

The amount of intrinsic damping in a structure depends on factors such as material, design, age, and condition, and it typically increases with vibration amplitude and frequency – all of which make intrinsic damping difficult to calculate. Alternatively, it must be measured or estimated from experience. As an order of magnitude, the intrinsic damping ratio is typically between one and two percent in steel structures, and between two and five percent in reinforced concrete structures. Since the structure of the Arecibo telescope is unique and is composed of both steel and concrete, its intrinsic damping ratio would be expected to be in a range between one and five percent.

Although we did not find any record of damping measurements for the telescope structure, damping can be estimated from the tiedown tensions recorded during the first cable failure on August 10, 2020. The tiedowns were equipped with load cells, and the tiedown tensions were logged every second. The tiedown tension data shows that the sudden release of the M4N cable tension acted as an impulsive load on the structure and triggered global vibrations that gradually diminished over several minutes due to damping. Because the tiedowns of the upgraded telescope are vertical cables between the platform corners and the ground, the tiedown tensions are proportional to the vertical movement of the platform corners. As shown in section 6.0 below, the first global dynamic mode of the structure involves such movement.

Each of the three platform corners had two tiedown cables, and each tiedown cable tension was measured independently. Platform corner 12 dropped approximately two feet when the M4N cable failed, causing its tiedown cables to become slack, while the tiedown cables at platform corners 4 and 8 remained taut (Figure 8). The tiedown cable tensions after failure are shown in Figure 9. The tensions were recorded once every second, with the periods of the vertical vibration of the platform expected to be in the order of three seconds (section 6.0 below). As a result, the vibration cycles are visible in the recorded cable tensions, but the peak cable tensions are not captured for every cycle. As shown in Figure 9, by fitting a logarithmic decrement to each recorded cable tension to estimate damping, we obtain a damping ratio of 1.0 percent from the corner 4 tiedown cables and 1.4 percent from the corner 8 tiedown cables. Based on these results, we assumed a damping ratio of one percent for every global vibration mode of the telescope structure in our dynamic analyses.

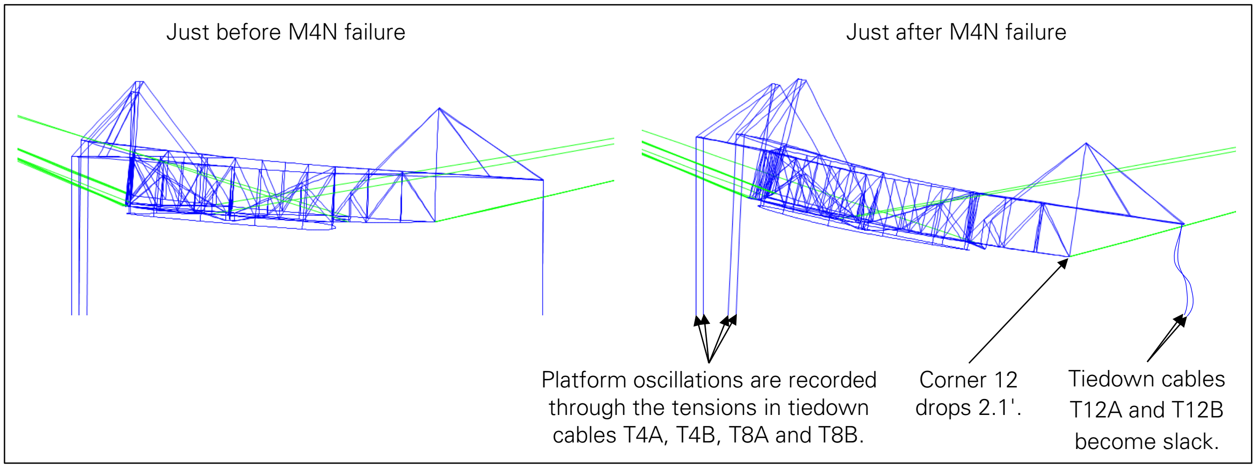

Figure 8: Platform response to M4N failure (looking west, displacements magnified x10).

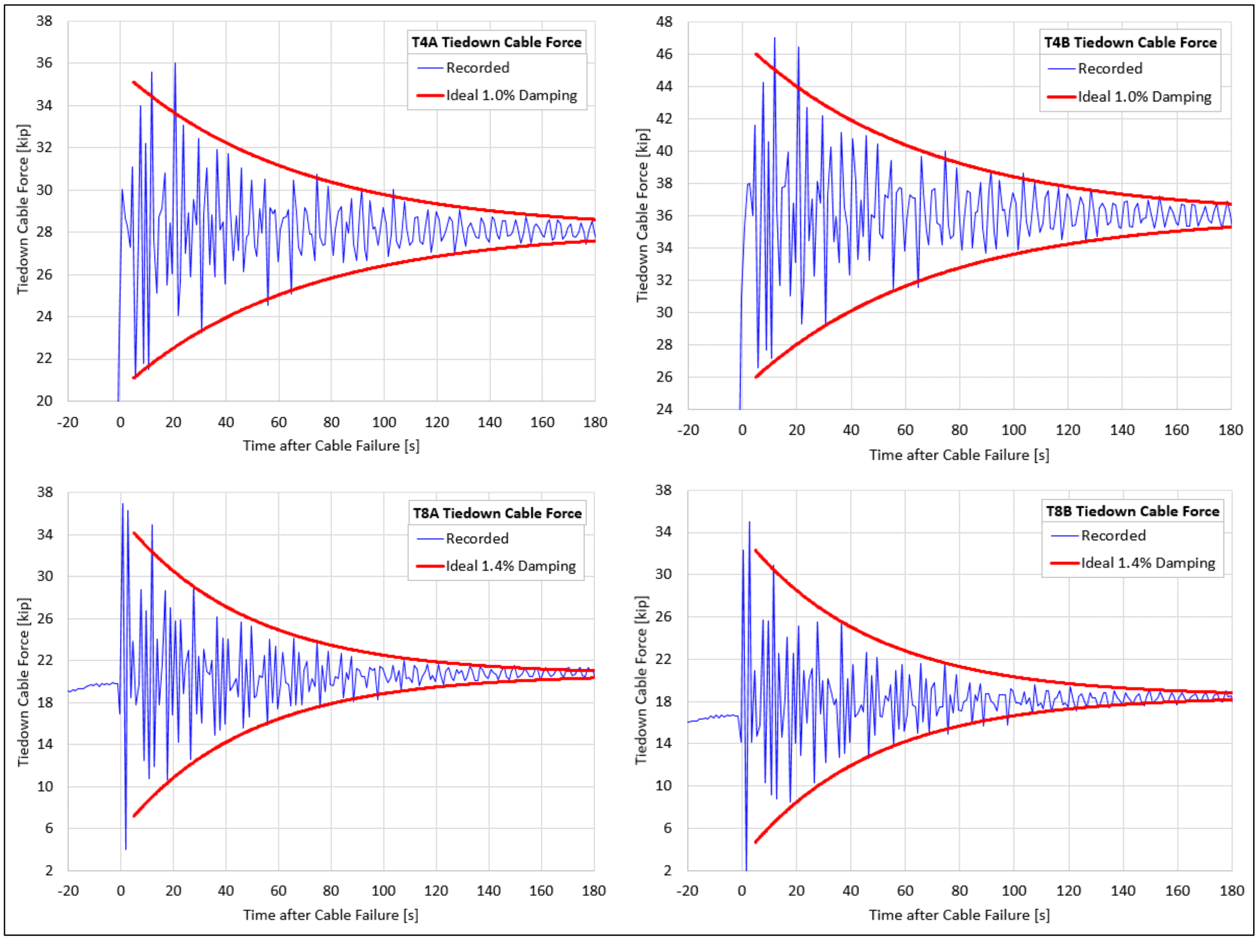

Figure 9: Damping measurement from tiedown tensions during first cable failure.

2.7 Summary of Model Baseline States

Before performing any analysis, the original and upgraded telescope models are initialized in the baseline states summarized in Table 5. Starting from a baseline state, analyses were performed by adding and/or tensioning the tiedowns, applying environmental loads, or moving the azimuth arm, Gregorian and/or line feeds. These analyses are presented in Appendix G, H, I, J and K.

Table 5: Summary of FE model baseline states.

	Original Structure	Upgraded Structure
Suspended Structure Weight	1,225 kip	1,825 kip
Cable Tensions	Specified at start of cable jacking sequence for second upgrade.	Determined through analysis from August 2020 cable sag survey.
Telescope Position	Stowed	Stowed
Tiedowns	Removed	Slack
Damping Ratio	1%	1%

3.0 SAP2000 Models

SAP2000 is a finite element analysis program developed by Computers and Structures and commonly used for structural analysis in the industry. SAP2000 is particularly effective at analyzing structures made of discrete slender members, such as building frames and steel bridges, and can account for geometric nonlinearities, including large structural deformations and member P-delta effects.

The towers and suspended structure are modeled with SAP2000's *frame* element, which captures axial, shear, bending and torsional stresses and strains. The mains and backstays are modeled with SAP2000's *cable* element. It is a nonlinear element that captures the changing direction of the tension with the cable curvature, and considers the cable stiffness reduction due to sag. The behaviors of the frame and cable elements are compared in Figure 10.

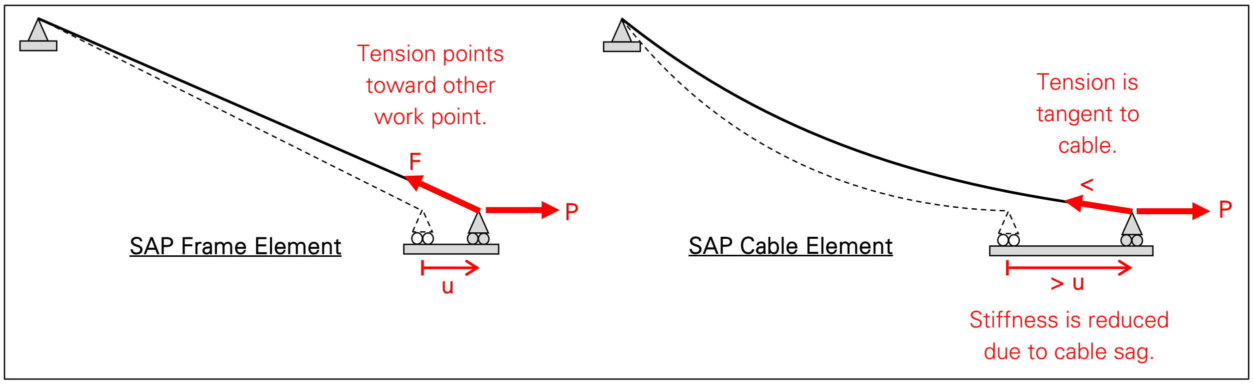

Figure 10: Frame vs. cable element for cable modeling in SAP2000.

SAP2000 is efficient to set up and run a large number of analyses in a given model, which facilitates the telescope analysis for different positions of the azimuth arm, Gregorian and/or line feed(s), with wind or earthquakes of different magnitude coming from different directions. For this purpose, we used SAP2000 models as the main production models for the analysis of the Arecibo structure. Every cable tension analysis presented in this report was performed using a SAP2000 model. As detailed below in section 4.0, some of the analyses were replicated in Abaqus to verify the SAP2000 results.

Overviews of the SAP2000 models were previously shown in Figure 1 and Figure 2.

4.0 Abaqus Models

Abaqus is a general-purpose finite element analysis program developed by Dassault Systems, which is commonly used in the industry and academia for a variety of applications far beyond the analysis of structures. As a top-of-the-line finite element analysis program with a strong validation record, Abaqus can access an extensive library of elements and material models to analyze a broad range of problems for structural analysis.

The telescope towers and suspended structure are modeled with Abaqus' *B31* element – a standard 2-node linear element with essentially the same behavior characteristics as SAP2000's *frame* element. The mains and backstays are modeled with Abaqus' *B31H* element, which accounts for the changing direction of the tension with the cable curvature, but not for the cable stiffness reduction due to sag (Figure 11).

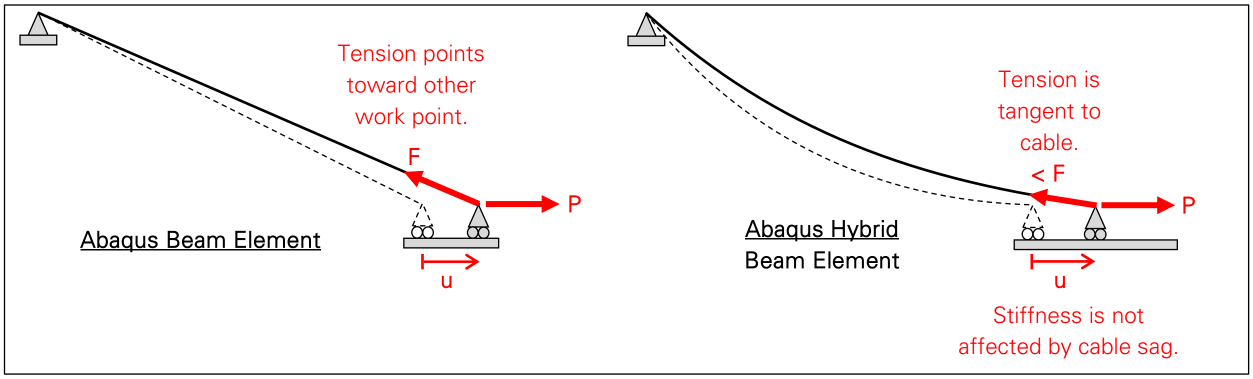

Figure 11: Beam vs. hybrid beam element for cable modeling in Abaqus.

The telescope's cable stiffness reduction due to cable sag is detailed in Table 6. The maximum reduction of 1.7 percent has a minimal impact on the results and conclusions of any cable tension analysis, so Abaqus' *B31H* element is appropriate for modeling the telescope cables.

We used the Abaqus models as validation models for the primary analysis work performed in SAP2000.

Table 6: Cable axial stiffness reduction due to sag.

Cable	Axial Stiffness Neglecting Sag [kip/in]	Original Structure			Upgraded Structure		
		Average Tension [kip]	Axial Stiffness Considering Sag [kip/in]	Axial Stiffness Relative Change due to Sag	Average Tension [kip]	Axial Stiffness Considering Sag [kip/in]	Axial Stiffness Relative Change due to Sag
M4	19.10	480	18.87	-1.2%	494	18.89	-1.1%
M4N	18.32	-	-	-	576	18.01	-1.7%
M4S	18.32	-	-	-	640	18.10	-1.2%
M8	19.10	480	18.87	-1.2%	500	18.90	-1.1%
M8N	18.32	-	-	-	578	18.02	-1.7%
M8S	18.32	-	-	-	618	18.07	-1.4%
M12	19.10	480	18.87	-1.2%	483	18.87	-1.2%
M12E	18.32	-	-	-	605	18.06	-1.5%
M12W	18.32	-	-	-	647	18.10	-1.2%
B4	23.61	547	23.42	-0.8%	567	23.44	-0.7%
B4N	27.23	-	-	-	668	26.96	-1.0%
B4S	27.23	-	-	-	635	26.92	-1.2%
B8	30.43	504	30.20	-0.8%	528	30.23	-0.7%
B8N	34.47	-	-	-	592	34.10	-1.1%
B8S	34.47	-	-	-	582	34.08	-1.1%
B12	28.27	520	28.09	-0.7%	561	28.12	-0.5%
B12E	32.14	-	-	-	715	31.95	-0.6%
B12W	32.14	-	-	-	594	31.81	-1.0%

5.0 Global Mass and Stiffness

The suspended structure is flexible and its deformation under load is captured in the structural analysis models, with each steel member modeled as a flexible frame element. To perform order-of-magnitude calculations or validate complex analysis results, however, it can also be useful to consider the suspended structure as a rigid body that can move and rotate in three directions under the effect of loads (Figure 12), based on its mass and the stiffness provided by the supporting towers and cables. The relevant mass and stiffness properties are summarized in Table 7 and Table 8. The mass properties were determined analytically from the position and properties of the steel members and adding the contributions of the SDL, Gregorian, line feed(s) and/or counterweight. The moment of inertia about each axis assumes that the axis passes through the center of mass of the suspended structure. To determine the stiffness properties, we applied unit loads to the suspended structure and calculated its global displacement and rotation from the deflections observed at the three bottom corners of the platform. This was done without making the suspended structure rigid in the model, and with the azimuth arm, Gregorian and/or line feed(s) in stowed position.

General observations are as follows:

- The auxiliary cables, added during the second upgrade, increase the horizontal stiffness (translation in both horizontal directions) by 30 percent and the torsional stiffness (rotation about vertical axis) by 360 percent.
- The vertical stiffness (translation in vertical direction) of the upgraded structure is 250 percent greater when the tiedowns are taut than when they are slack.
- Despite having more support cables and vertical tiedowns, the upgraded structure has a slightly lower vertical stiffness (translation in vertical direction) than the original structure. This is because the tiedowns of the upgraded structure are connected to the platform through outriggers that add flexibility to the tiedown system.
- Most of the tilt stiffness (rotational stiffness about both horizontal axes) is provided by the tiedowns, as shown by the relatively low tilt stiffness values for the upgraded structure with tiedowns slack.

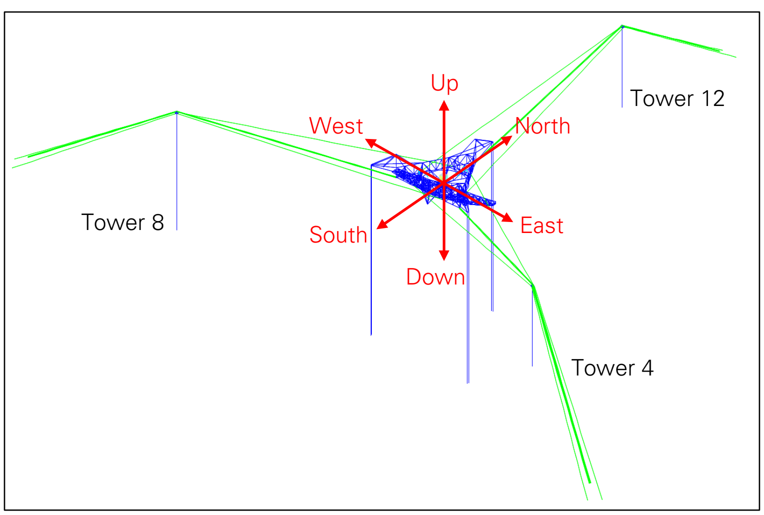

Figure 12: Suspended structure axes.

Table 7: Global mass properties of suspended structure, in stowed position.

		Original Structure	Upgraded Structure
Weight [kip]		1,225	1,825
Mass [kip·s^2/ft]		38.0	56.7
Moment of inertia [kip·ft·s^2/deg]	North-South Axis	2,674	4,177
	East-West Axis	1,640	2,193
	Vertical Axis	3,677	5,078

Table 8: Global stiffness properties of suspended structure.

		Original Structure	Upgraded Structure with Tiedowns Slack	Upgraded Structure with Tiedowns Taut
Translational stiffness [kip/ft]	North-South Axis	897	1,173	1,175
	East-West Axis	898	1,177	1,179
	Vertical Axis	340	119	297
Rotational stiffness [kip·ft/deg]	North-South Axis	64,342	22,414	79,251
	East-West Axis	64,399	22,904	79,767
	Vertical Axis	36,802	133,214	136,640

6.0 Dynamic Modes

The dynamic modes of a structure describe how the structure tends to vibrate in response to dynamic loads. The actual response of the structure may follow one or just a few modes when the load remains close to periodic over a long period of time, but the superposition of many modes may occur when the load is more random. In any case, knowing the dynamic modes is useful for interpreting and verifying the results of dynamic analysis. Prior to performing the wind and seismic analyses presented in Appendix J and K, we determined the modes of the telescope from the SAP2000 and Abaqus models.

The modes of the original and upgraded structures are discussed in this section. For the upgraded structure, we consider cases where the tiedowns are tensioned or slack, since tiedowns were partially or fully loosened before windstorms. All of the modes assume that the telescope is in the pre-storm stowed position. In the figures showing the mode shapes, we have highlighted the greatest displacements for each mode. For practical purposes, only the modes with a period greater than 1 second are shown in this appendix.

General observations about the modes are as follows:

- Most of the modes involve bending of one or several towers. The towers are therefore integral to dynamic analysis, and cannot be considered as fixed supports for the suspended structure.
- Multiple modes involve the rotation of the suspended structure about a vertical axis, or about an axis parallel or perpendicular to the azimuth arm. These modes are partially driven by the masses of the Gregorian and line feed(s) being at a distance from the axis of rotation, and therefore these modes depend on the position of the azimuth arm, Gregorian, and line feed(s). All of the modes illustrated below assume that the telescope is stowed, but we expect that modes of similar periods and shapes would be obtained for other configurations of the telescope.

6.1 Original Structure

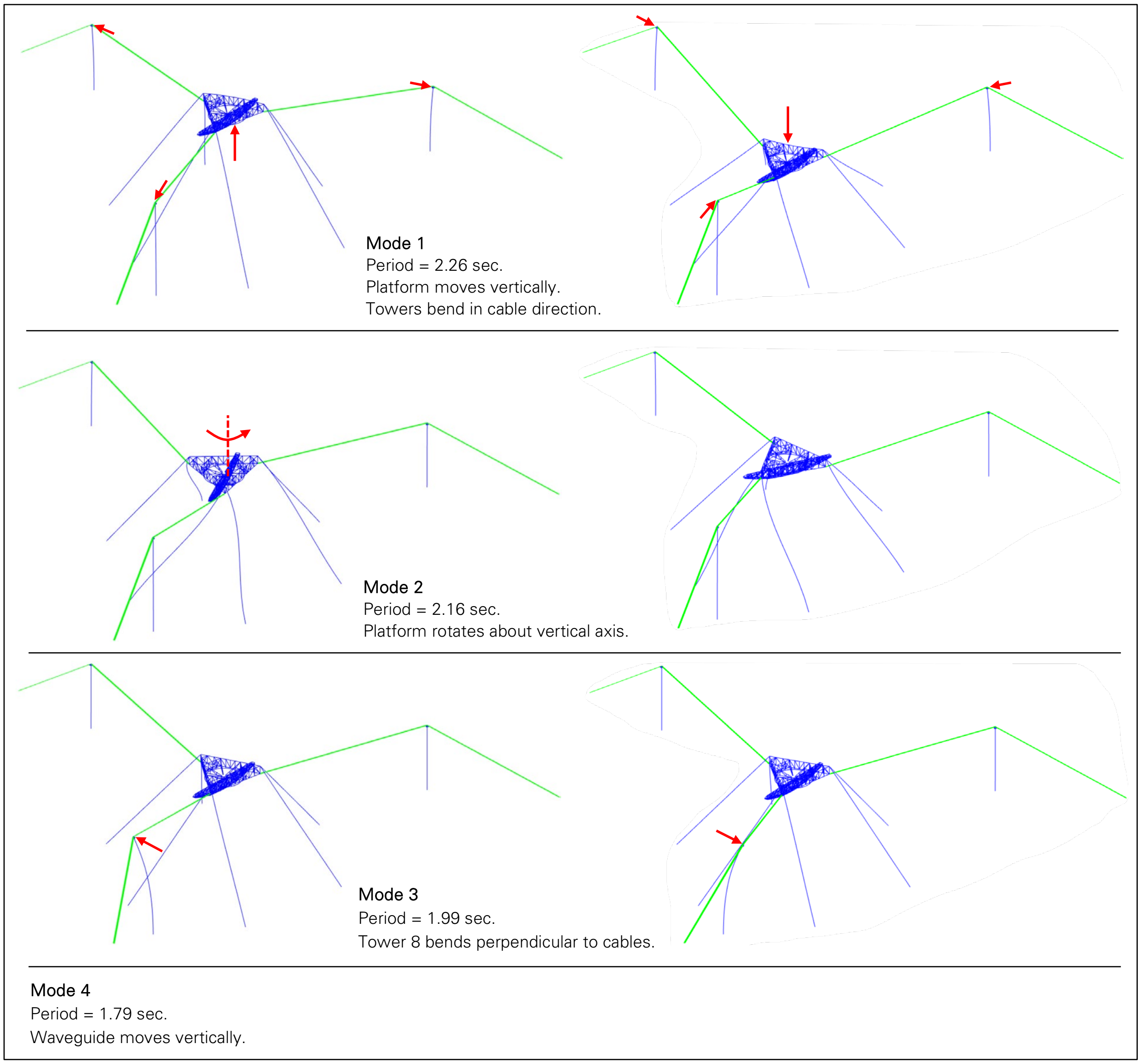

Figure 13: Vibration modes 1-4 of original structure.

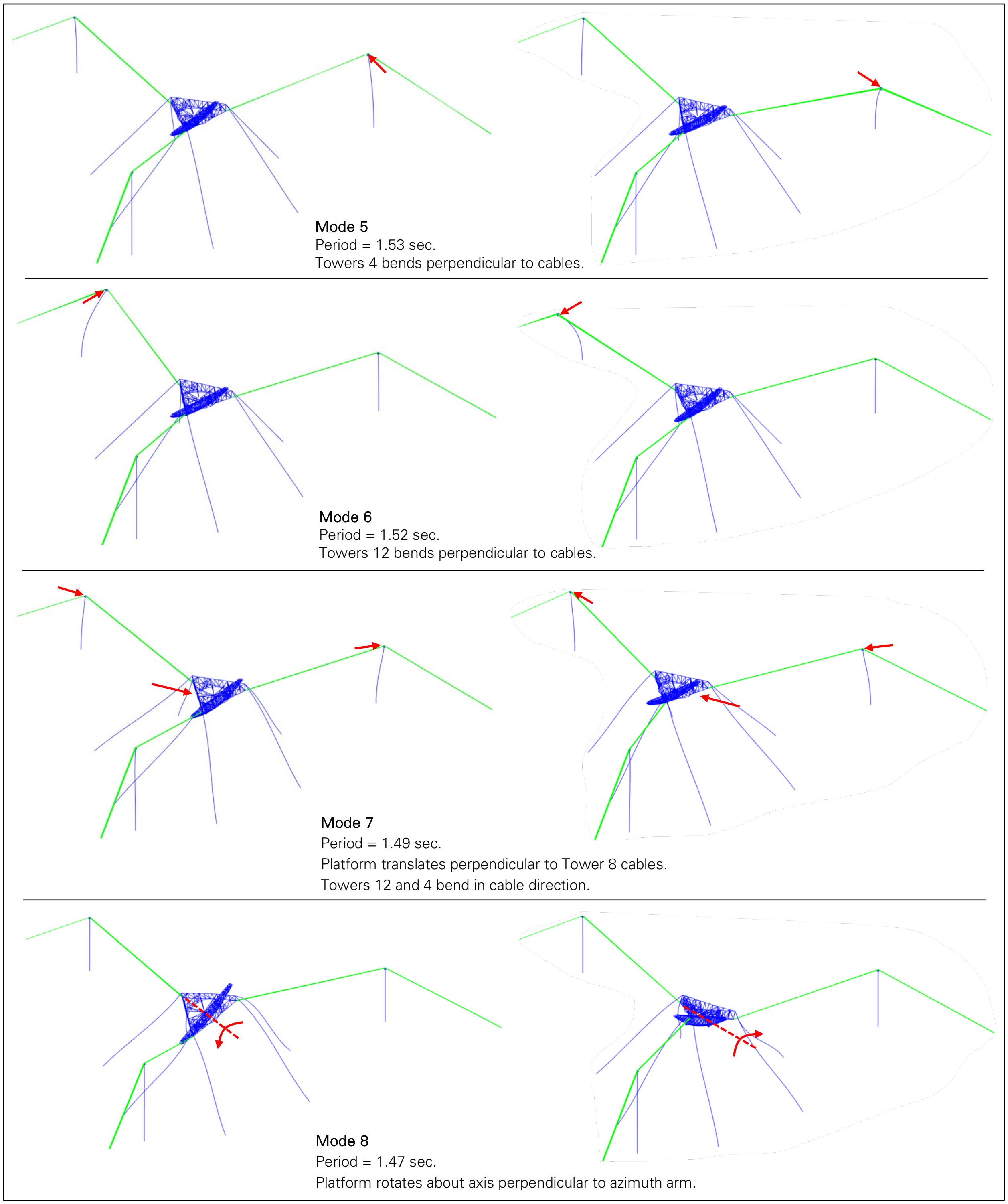

Figure 14: Vibration modes 5-8 of original structure.

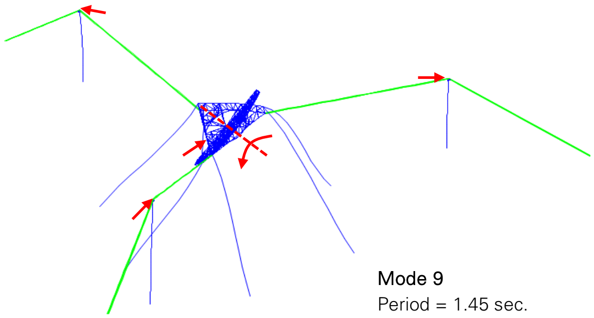
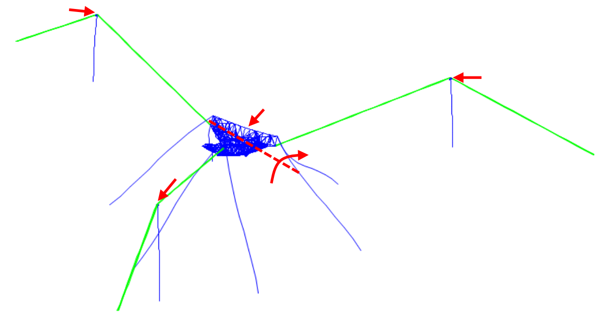

Mode 9
Period = 1.45 sec.
Platform rotates about axis perpendicular to azimuth.
Platform translates in Tower 8 cable direction.
Towers bend in cable direction.

Mode 10
Period = 1.25 sec.
Waveguide moves horizontally.

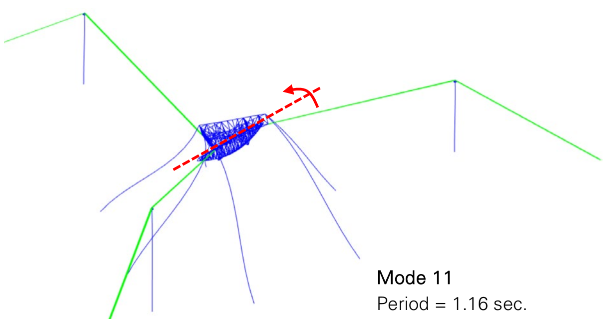
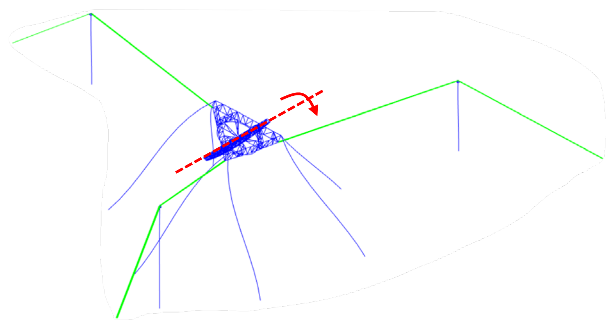

Mode 11
Period = 1.16 sec.
Platform rotates about axis parallel to azimuth arm.

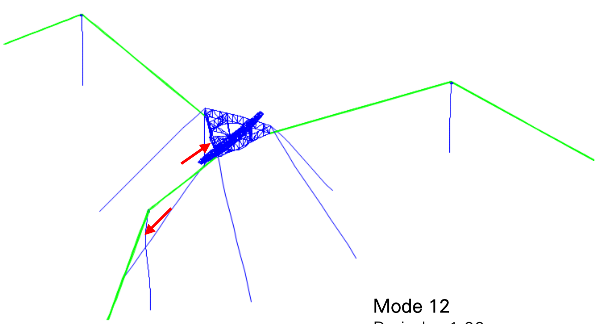
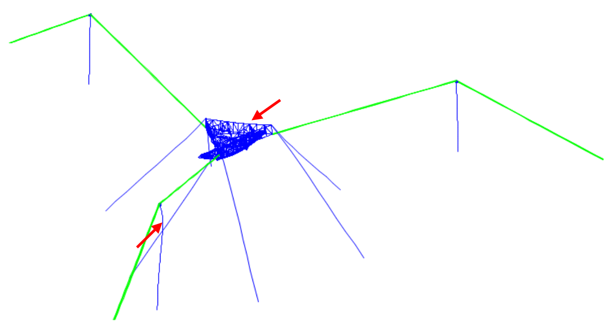

Mode 12
Period = 1.00 sec.
Platform translates parallel to M8 Cables.
Tower 8 sees 2nd mode bending in cable direction.

Figure 15: Vibration modes 9-12 of original structure.

6.2 Upgraded Structure

6.2.1 Tiedowns Tensioned

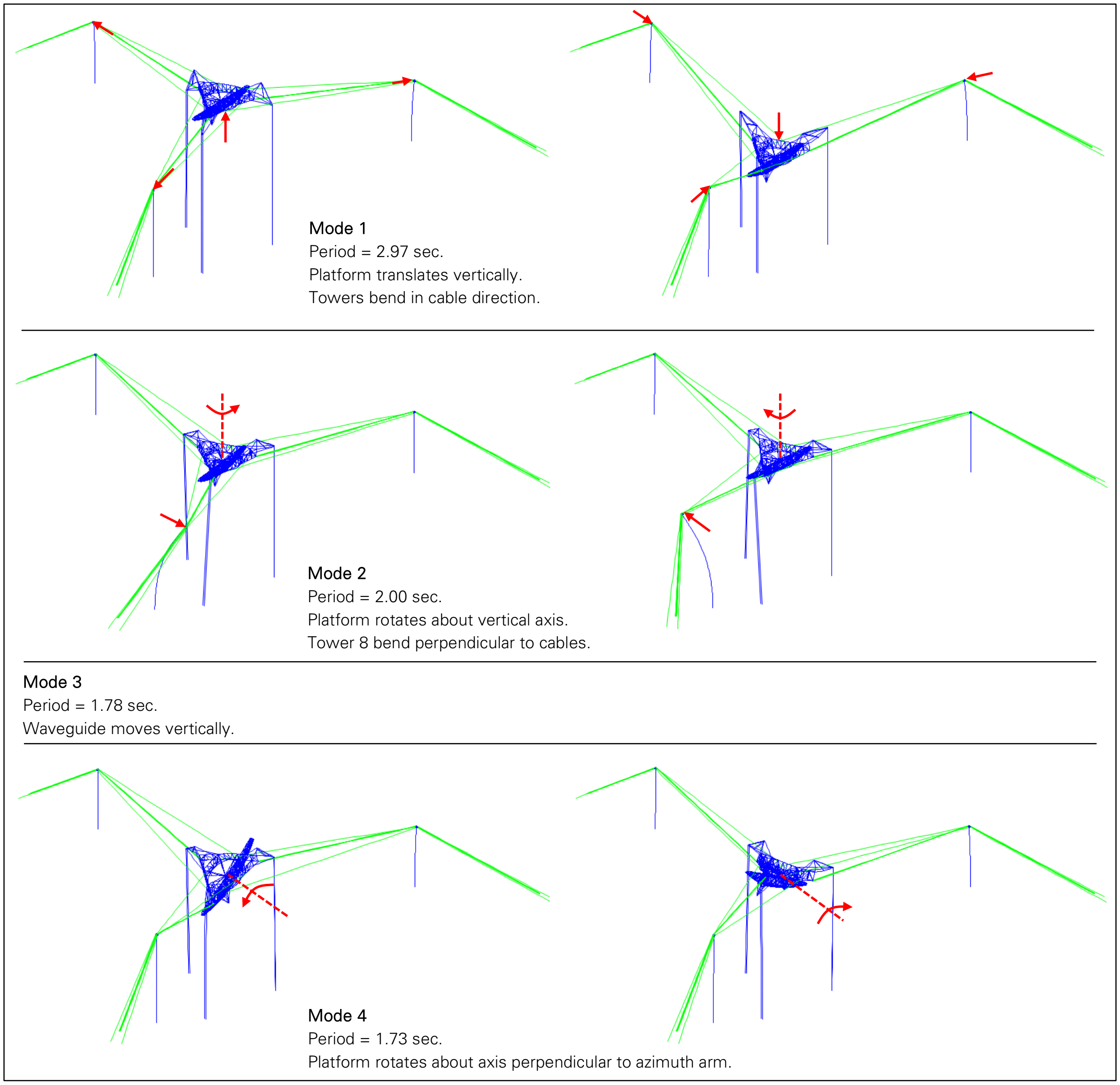

Figure 16: Vibration modes 1-4 of upgraded structure with tiedowns tensioned.

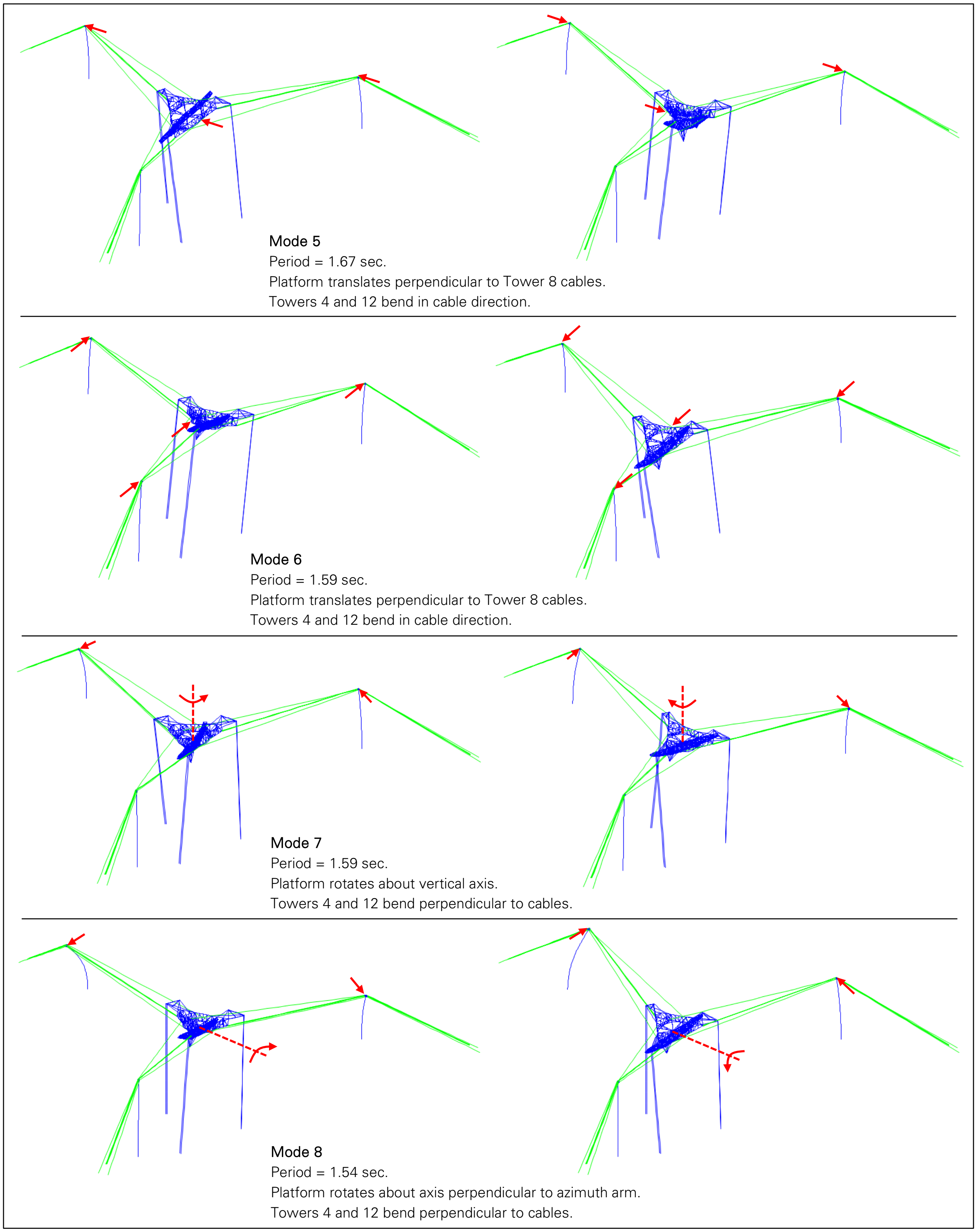

Figure 17: Vibration modes 5-8 of upgraded structure with tiedowns tensioned.

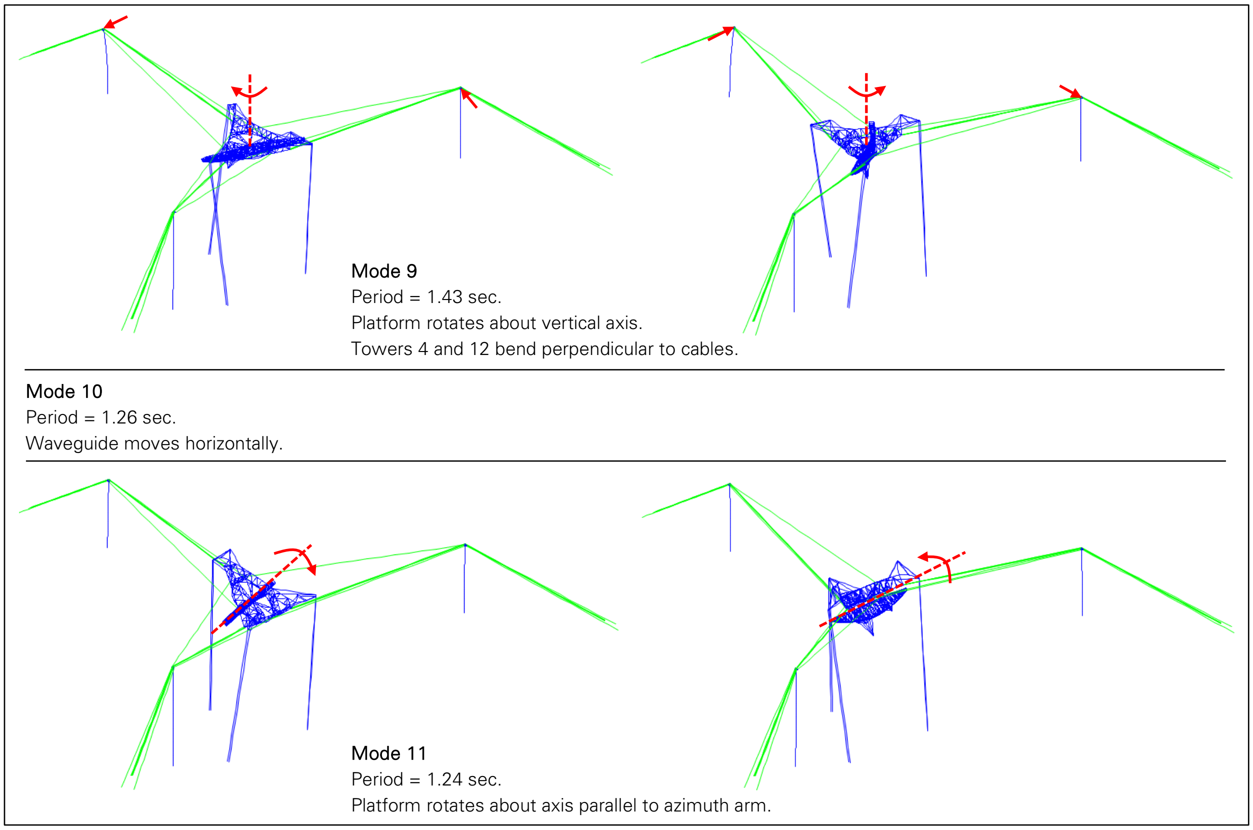

Figure 18: Vibration modes 9-11 of upgraded structure with tiedowns tensioned.

6.2.2 Tiedowns Slack

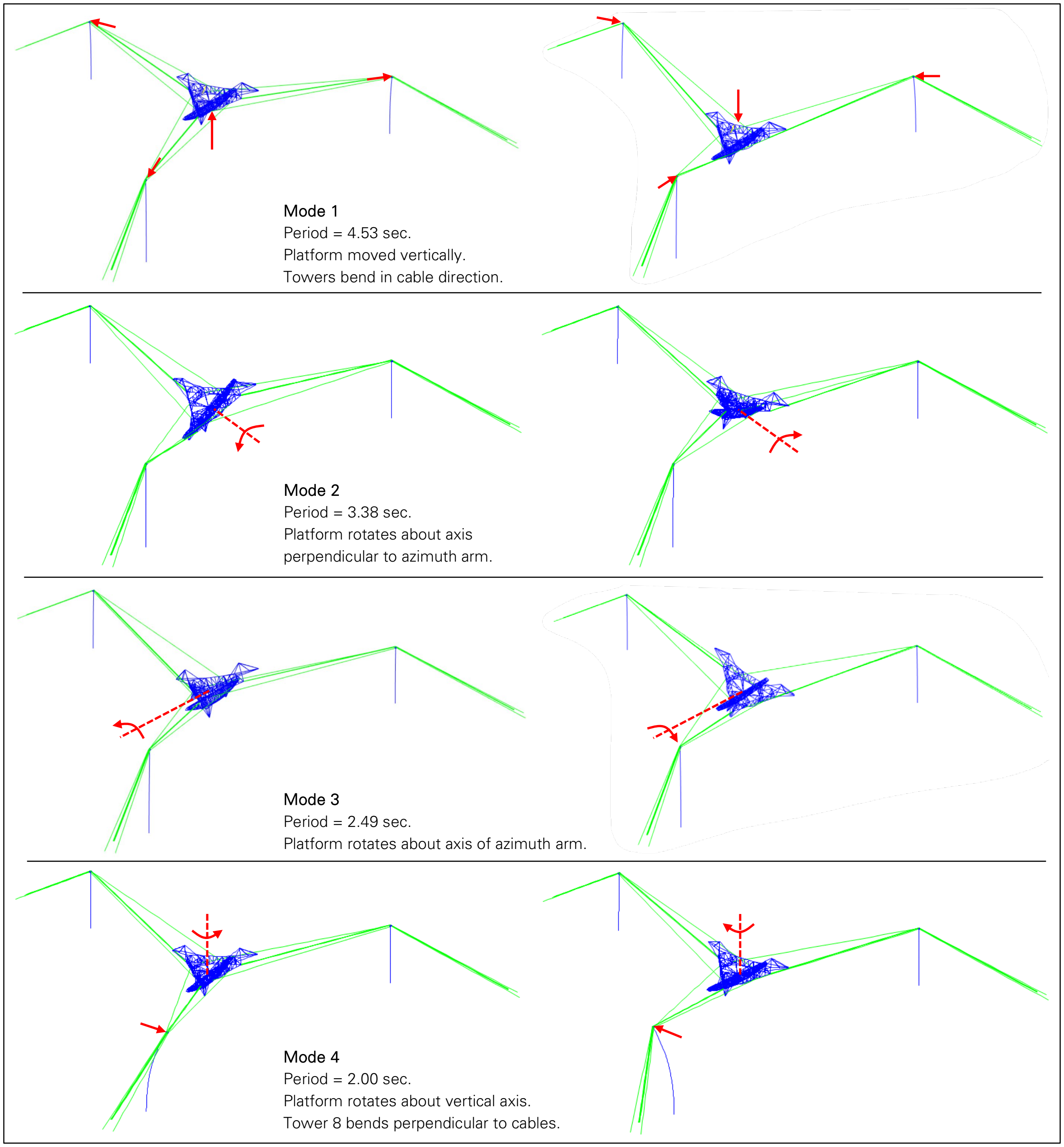

Figure 19: Vibration modes 1-4 of upgraded structure with tiedowns slack.

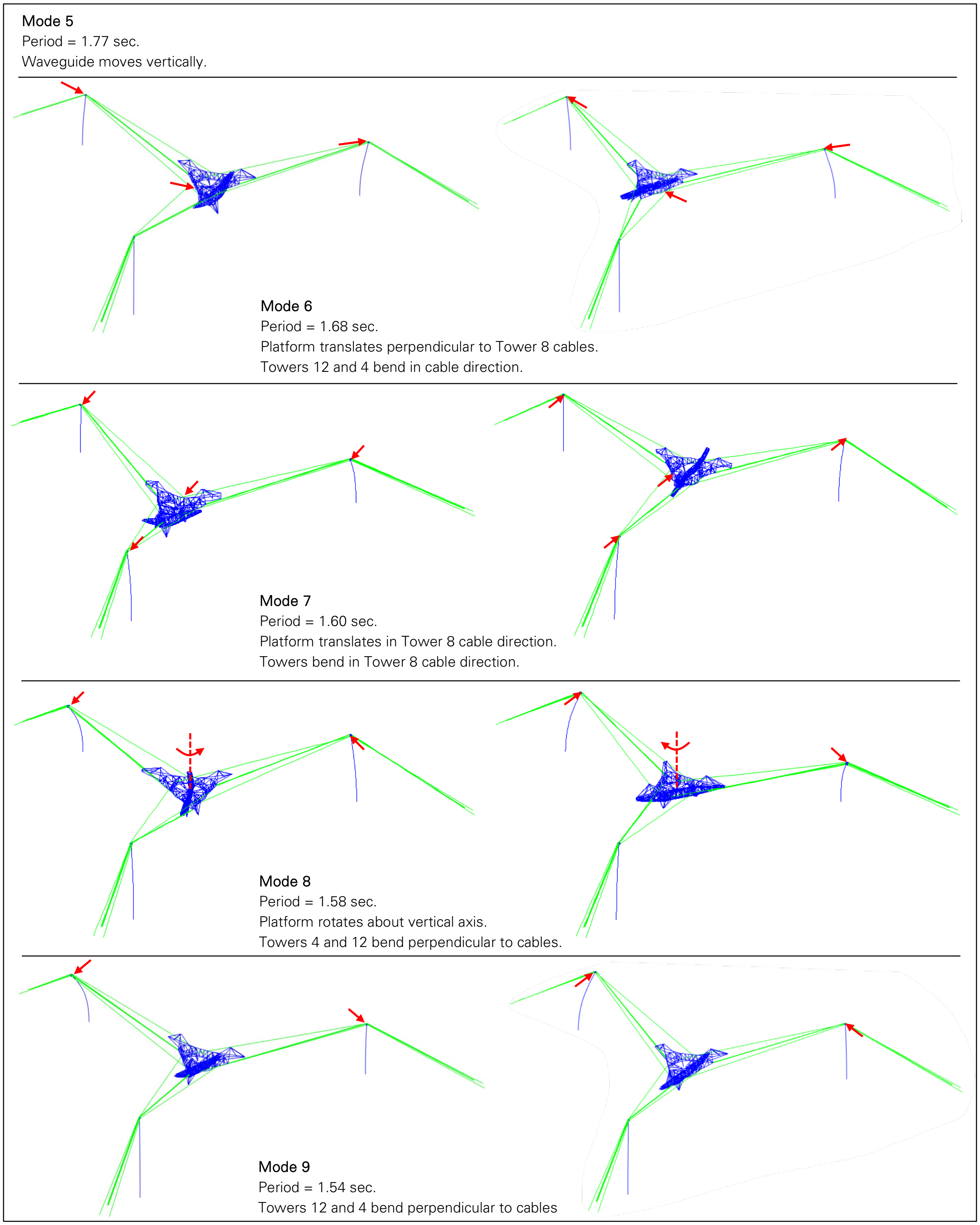

Figure 20: Vibration modes 5-9 of upgraded structure with tiedowns slack.

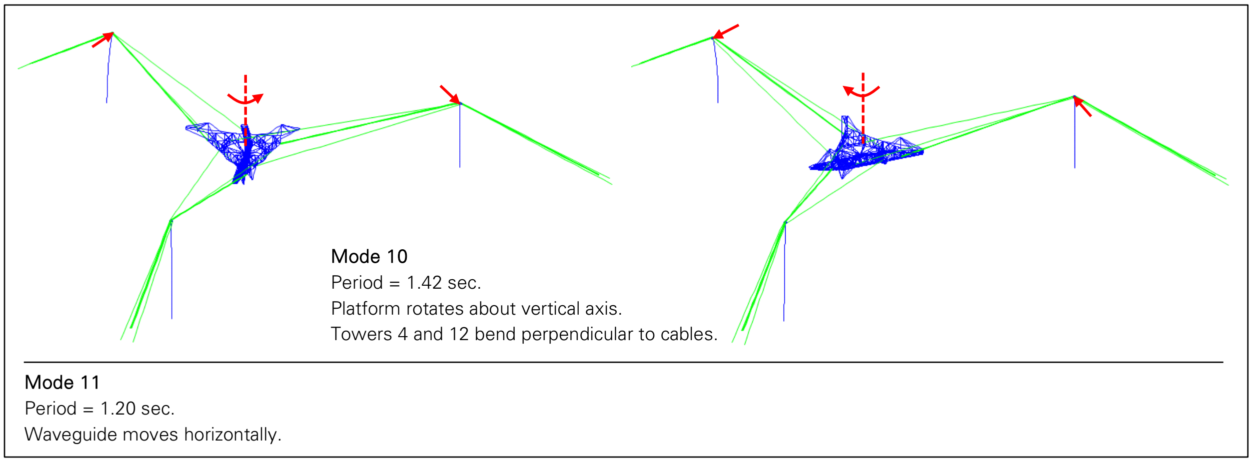

Figure 21: Vibration modes 10-11 of upgraded structure with tiedowns slack.